Topographical mapping of α- and β-keratins on developing chicken skin integuments: Functional interaction and evolutionary perspectives

Ping Wu[a,1], Chen Siang Ng[b,1], Jie Yan[a,c], Yung-Chih Lai[a,d,e], Chih-Kuan Chen[b,f], Yu-Ting Lai[b], Siao-Man Wu[b], Jiun-Jie Chen[b], Weiqi Luo[a], Randall B. Widelitz[a], Wen-Hsiung Li[b,g,2], and Cheng-Ming Chuong[a,d,e,h,2]

[a]Department of Pathology, Keck School of Medicine, University of Southern California, Los Angeles, CA 90033; [b]Biodiversity Research Center, Academia Sinica, Taipei 11529, Taiwan; [c]Jiangsu Key Laboratory for Biodiversity and Biotechnology, College of Life Sciences, Nanjing Normal University, Nanjing 210023, China; [d]Research Center for Developmental Biology and Regenerative Medicine, National Taiwan University, Taipei 10041, Taiwan; [e]Integrative Stem Cell Center, China Medical University, Taichung 40447, Taiwan; [f]Institute of Ecology and Evolutionary Biology, National Taiwan University, Taipei 10617, Taiwan; [g]Department of Ecology and Evolution, University of Chicago, Chicago, IL 60637; and [h]Center for the Integrative and Evolutionary Galliform Genomics, National Chung Hsing University, Taichung 40227, Taiwan

Contributed by Wen-Hsiung Li, October 19, 2015 (sent for review July 19, 2015; reviewed by Scott V. Edwards and Roger H. Sawyer)

Avian integumentary organs include feathers, scales, claws, and beaks. They cover the body surface and play various functions to help adapt birds to diverse environments. These keratinized structures are mainly composed of corneous materials made of α-keratins, which exist in all vertebrates, and β-keratins, which only exist in birds and reptiles. Here, members of the keratin gene families were used to study how gene family evolution contributes to novelty and adaptation, focusing on tissue morphogenesis. Using chicken as a model, we applied RNA-seq and in situ hybridization to map α- and β-keratin genes in various skin appendages at embryonic developmental stages. The data demonstrate that temporal and spatial α- and β-keratin expression is involved in establishing the diversity of skin appendage phenotypes. Embryonic feathers express a higher proportion of β-keratin genes than other skin regions. In feather filament morphogenesis, β-keratins show intricate complexity in diverse substructures of feather branches. To explore functional interactions, we used a retrovirus transgenic system to ectopically express mutant α- or antisense β-keratin forms. α- and β-keratins show mutual dependence and mutations in either keratin type results in disrupted keratin networks and failure to form proper feather branches. Our data suggest that combinations of α- and β-keratin genes contribute to the morphological and structural diversity of different avian skin appendages, with feather-β-keratins conferring more possible composites in building intrafeather architecture complexity, setting up a platform of morphological evolution of functional forms in feathers.

skin appendage | feather | scale | claw | beak | Evo-Devo

The integument mediates interactions between an organism and its environment. It serves as the first line of defense against external factors, such as physical injuries, pathogens and provides insulation, sensation, and locomotion (1–3). The integument includes not only the epidermis and dermis, but also integumentary derivatives, namely invaginated glands and protruded appendages, such as hairs, feathers, and teeth (3, 4). Integumentary derivatives represent the integration of many evolutionary steps that combine to form diverse structural variations, allowing animals to adapt to various ecospaces according to their specific lifestyles (3).

The evolution of a gene family may contribute to phenotypic evolution (5, 6), due to changes in the protein sequence, gene copy number, or temporal and spatial expression patterns of duplicated genes. The avian feather provides an excellent model for studying how the evolution of gene families can contribute to the emergence and diversification of novel structures in animals (4, 7, 8). Feathers are mainly composed of α- and β-keratins. The former are found in all vertebrates, whereas the latter only in birds and reptiles (9–11). A recent study found that regulatory innovations of feather development genes predate the origin of feathers, suggesting that the avian dinosaur ancestor already had the nonkeratin protein-coding toolkit for making feathers (12). While fewer new genes have been found in bird genomes (13) and the α-keratin gene family has shrunk in birds relative to mammals and reptiles (14, 15), the expansion of β-keratin genes is one of the most unique genomic features of birds (13, 14).

Feathers and scales may share the initial epidermal placode structure as a basal feature for the formation of epidermal appendages. From here, feathers and scales diverge. Novel morphogenetic processes have evolved, leading to the complex feather morphology and make feathers and scales distinct in their mature structures (16–18). Recently, molecular networks for the multistep evolution of novel pathways, which exist in feather but not scale morphogenesis, have been identified and reviewed (19). They involved the recruitment of signaling pathways such as the FGF (fibroblast growth factor), BMP (bone morphogenetic protein) and Wnt (wingless-integration) pathways as well as adhesion

Significance

Avian skin appendages include feathers, scales, claws, and beaks. They are mainly composed of α-keratins, found in all vertebrates, and β-keratins, found only in birds and reptiles. Scientists have wondered how keratins are interwoven to form different skin appendages. By studying keratin gene expression patterns in different chicken skin appendages, we found α- and β-keratin interactions crucial for appendage morphogenesis. Mutations in either α- or β-keratins can disrupt keratin expression and cause structural defects. Thus, different combinations of α- and β-keratins contribute to the structural diversity of feathers. The expansion of β-keratin genes during bird evolution might have greatly increased skin appendage diversity because it increased the possible interactions between α- and β-keratins.

Author contributions: P.W., C.S.N., W.-H.L., and C.-M.C. designed research; P.W., J.Y., Y.-T.L., S.-M.W., J.-J.C., and W.L. performed research; Y.-C.L. and C.-K.C. analyzed data; and P.W., C.S.N., R.B.W., W.-H.L., and C.-M.C. wrote the paper.

Reviewers: S.V.E., Harvard University; and R.H.S., University of South Carolina.

The authors declare no conflict of interest.

Data deposition: The genome reads reported in this paper have been deposited in the NCBI BioProject database, www.ncbi.nlm.nih.gov/bioproject (accession no. PRJNA285133) and the full datasets have been submitted to the NCBI BioSample database, www.ncbi.nlm.nih.gov/biosample (accession nos. SAMN03738256–SAMN03738262).

[1]P.W. and C.S.N. contributed equally to this work.

[2]To whom correspondence may be addressed. Email: whli@uchicago.edu or cmchuong@usc.edu.

This article contains supporting information online at www.pnas.org/lookup/suppl/doi:10.1073/pnas.1520566112/-/DCSupplemental.

molecules (7, 8, 20) for feather morphogenesis. Feather forming steps include the formation of follicle structure (21), cyclic regeneration of feather stem cells (22), and branching morphogenesis (23).

Furthermore, comparative genomic studies showed that the number of α- and β-keratin genes and β-keratin gene diversity were important for feather evolution and the adaptation of birds to diverse ecological niches (13, 14, 24, 25). Apparently, compositional changes of keratins are associated with different avian lifestyles. A new subfamily of β-keratin genes, the feather-β-keratin genes, has evolved to form a fiber-like structure, in contrast to the scale- and claw-β-keratins that form interweaving filament bundles (9, 11, 26). Feather-β-keratins might have evolved from scale-β–keratins by losing the glycine and tyrosine-rich tail moieties, conferring more flexibility to feathers compared with the rigid scales and claws of birds. Because some dinosaurs have been shown to have feathers, it is reasonable to assume that some kinds of feather-like β-keratins were already present in feathered dinosaurs (24). However, molecular dating studies show that the basal β-keratins of birds began diverging from their archosaurian ancestor earlier than 200 Mya (million years ago). But, the subfamily of feather-β-keratins, as found in living birds, did not begin to diverge until approximately 143 Mya (27). These findings combine to suggest it is likely that avian dinosaur ancestors might have evolved some primitive types of β-keratin to make their ancient feathers. As time goes on, more complex "feather-β-keratin genes" emerge, later than the origin of feathers. The diversification of the newly evolved feather-β-keratins were apparently crucial for birds to evolve various feather types with better performance in properties such as thermoregulation and aero-engineered flight. Such new features have allowed birds to adapt into various ecological niches quickly (19, 28) and become the most diversified terrestrial vertebrates.

The discrepancy of evolution timing in the morphogenesis and keratin differentiation of feathers in dinosaurs and birds make it interesting and essential to understand β-keratin evolution at the genomic level. Indeed, the study of feather evolution and function has been hindered by the scarcity of keratin expression data. Some earlier work was done to detect β-keratin expression by in situ hybridization (9, 29). With recent advances in chicken genome research, we are now able to generate specific probes to investigate detailed expression patterns of α- and β-keratin genes in feathers, scales, claws, and beaks. Note that a feather consists of many elaborate structural parts that differ in mechanical properties and functions. Our previous study revealed that different α- and β-keratins are differentially expressed in different parts of a contour or flight feather (25). Moreover, using the avian RCAS transgenic system to express mutated α-keratin genes in adult chicken feather follicles, we showed that α-keratins play an important role in feather structure.

While the above work revealed the importance of α-keratins in adult chicken feathers, a systemic mapping of α- and β-keratin members onto different body regions, different skin appendages, and different structural components within an appendage remains to be carried out. In this study, we conducted topographic mapping of α- and β-keratin genes to skin appendages including feather, scutate scale, reticulate scale, claw, and beak, using the new keratin gene annotation in the current chicken genome assembly (Galgal4) (25). We used RNA-seq to examine the differential expression of α- and β-keratin genes in different developing integumentary organs, using their newly available gene annotation. We used specific probes targeting the 3′ UTR of genes that are generally not conserved among paralogs to demonstrate that in different skin appendages, many α-keratin and β-keratin genes are differentially expressed with body region specificity and intra-appendage differences via section in situ hybridization (SISH). Furthermore, using mutant or antisense RNA forms to modulate keratin gene expression, we demonstrated functional interdependence of α- and β-keratins during skin appendage morphogenesis. The topographical mapping of α- and β-keratins on the integument showed striking expression dynamics of β-keratins within the feather structures. This observation may have an implication for feather evolution that adapted feathered dinosaurs and birds to the sky (28).

Results

The Structure of Different Skin Appendages. We focused our mapping study to five skin appendages in developing chicken embryos from embryonic day (E)12 to E16 (Hamburger and Hamilton Stage 38–42; ref. 30). These skin appendages include beaks, feathers, scutate scales, reticulate scales, and claws (Fig. S1*A* and Fig. 1 *A–E*, *Left*). The basic epidermal components in different embryonic skin appendages include the periderm (PD), stratum basal (SB), stratum intermedium (SI), and stratum corneum (SC) (Fig. S1 *B–F*). However, each skin appendage has its own specific characteristics. We used schematic drawings (Fig. 1 *A–E*) and H&E staining of E12 (stage 38), E14 (stage 40), and E16 (Stage 42) (Fig. S2 *A–E*, *Left*) to demonstrate the characteristics of each appendage.

Beaks not only display upper beak (UB) and lower beak (LB) differences, but also have outer-oral and inner-oral differences (Fig. 1*A*). In addition, the upper beak has a thick periderm (PM) and an egg tooth (Et) structure (Fig. S1*B* and Fig. 1*A*). By E12, these basic beak structures have already been established (Fig. S2*A*). Feathers are considered to represent the most complex skin appendages in vertebrates and have a hierarchical branched morphology (18, 31). Along the proximal-distal axis, the epidermis gradually differentiates to form barb ridges, which include the barbule plate (BP), marginal plate (MP), and axial plate (AP) (Fig. S1*C* and Fig. 1*B*). The barbule plate will become the final feather barbule. The inner part of the barb ridge, closest to the pulp, will differentiate to form the ramus (the branch with barbules on it) to produce embryonic downy feathers (31). The ramus is composed of medullary cells surrounded by barb cortical cells (1). At E12, the feather filament has these basic structures (Fig. S2*B*).

The structure of the overlapping scutate scales includes the outer surface (OS), the inner surface (IS), and the hinge (Hg) (Fig. 1*C*). The morphogenesis of the overlapping structure begins at E12 and matures at E16 (Fig. S2*C* and Fig. 1*C*). The layers of embryonic scale epidermis include the periderm, subperiderm (SP), stratum intermedium (SI), and stratum basal (SB) (1, 32, 33) (Fig. S1*D*). Previously, Sawyer and Knapp identified that the periderm could be divided into primary and secondary components (34). Here, we refer to both as a single entity. The periderm is an embryonic epidermis layer that will be shed before hatching (1). Morphological and immunohistochemical studies showed that scale subperiderm may be homologous with feather barb and barbule cells (34–37). The embryonic layers of scutate scales are shed at hatching, but their homologs may be retained in feathers (34–36), which remain to be investigated further.

Reticulate scales show left-right symmetry, but the surface and hinge regions differ in appearance; only the surface has papillary dermis structures (Fig. 1*D*). The dome shape of individual reticulate scales has not appeared by E12 (Fig. S2*D*), but is apparent by E14. Claws are asymmetric structures that display dorsal (unguis; Ug) and ventral (subunguis; Su) morphological differences (Fig. 1*E* and Fig. S1*F*). The dorsal-ventral difference has appeared at E12 (Fig. S2*E*).

To examine the temporal and spatial expression of keratin genes in different skin appendages, we used a common β-keratin gene probe to perform SISH. This probe is designed from the conserved coding region sequence among most β-keratin genes. The SISH data from E16 are shown in Fig. 1 *A–E*, *Right* and stainings from different stages are shown in Fig. S2. β-keratin genes are strongly expressed in the stratum intermedium of the

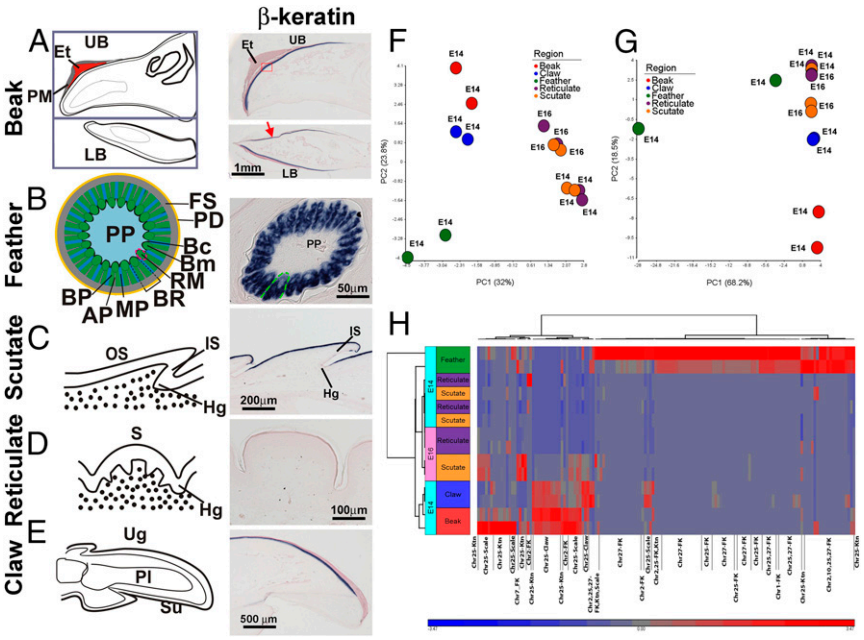

Fig. 1. Structures of avian skin appendages and RNA-seq analysis. (*A*–*E*) Schematic drawing (*Left*) and common β-keratin in situ hybridization (*Right*) of E16 embryonic skin appendages. (*A*) Beak. (*B*) Feather. (*C*) Scutate scale. (*D*) Reticulate scale. (*E*) Claw. Red arrow in *A* indicates expression of β-keratin in the oral epidermis. Green dotted line in *B* indicates the barb ridge. (*F* and *G*) Multidimensional scaling (MDS) plot of RNA-seq samples for α-keratin genes (*F*) and β-keratin genes (*G*). Similarities of gene expression patterns were calculated and mapped for E14 beaks, E14 feathers, E14 scutate scales, E14 reticulate scales, E14 claws, E16 scutate scales, and E16 reticulate scales. (*H*) Hierarchical clustering of β-keratin gene expression profile inferred from RNA-seq data; *Bottom* shows enriched subfamilies in each cluster. AP, axial plate; Bc, barb cortex; Bm, barb medulla; BP, barb plate; BR, barb ridge; Et, egg tooth; FS, feather sheath; Hg, hinge; IS, inner surface; LB; lower beak; MP, marginal plate; OS, outer surface; PD, periderm; PI, Phalange I; PM, periderm above the egg tooth; PP, pulp; RM, ramus; S, surface; Su, subunguis; UB, upper beak; Ug, unguis.

upper and lower beak from E12 to E16 (Fig. S2*A*, *Middle* and *Right*). However, the lower beak oral epidermis also expresses β-keratin genes at E16 (red arrow). β-keratin transcripts are detected at the tip of the feather filament at E12 (Fig. S2*B*). The β-keratin expression pattern in E14 and E16 feather follicles are similar. In both samples, β-keratin is expressed in the barbule plate (arrows) but absent in the future ramus region (red circle) (Fig. S2*B*). By E16, the feather has stronger staining and the unstained ramus area becomes smaller (Fig. S2*B*). β-keratin transcripts are absent in E12 scutate scales, faintly detected in E14, and become much stronger at E16, with a negative inner surface (Fig. 1*C* and Fig. S2*C*). The β-keratin transcripts could not be detected in E12, E14, or E16 reticulate scales (Fig. S2*D*). Claws have extensive β-keratin transcripts in the unguis, but these transcripts are absent from the subunguis at different stages, with the strongest and largest expression area present at E16 (Fig. 1*E* and Fig. S2*E*). These results demonstrate the temporal and spatial differences of β-keratin expression among different skin appendages and even within the same appendage.

Differential Expression of Keratin Genes in Different Skin Appendages. The temporal and spatial differences in β-keratin gene expression shown above for different skin appendages prompted us to examine the differential expression of keratin genes (both α- and β-keratin) in greater detail. We used RNA-seq to examine five different skin appendages at E14 (feathers, scutate scales, reticulate scales, claws, and beaks) (Table S1). Because β-keratin is expressed faintly in E14 scutate scales and was absent in E14 reticulate scales (Fig. S2 *C* and *D*), we conducted RNA-seq of E16 scutate scales and reticulate scales.

The RNA-seq data demonstrate that different skin appendages may use different α- and β-keratins to achieve their final form. When the 12,655 filtered genes were used to perform principal component analysis (PCA) for the 14 samples, Principal component 1 (PC1) correlates with tissue differences, whereas developmental stages of both scale types are resolved along PC2 (Fig. S3*A*). When PCA was performed only on α-keratin genes, duplicate samples cluster together nicely (Fig. 1*F*).

However, when β-keratin genes were used to generate a PCA plot, feather samples are separate from all other samples along PC1, whereas some scale samples from different scale types or from different embryonic ages cannot be resolved by PC2 (E14 scutate, E14 reticulate, and E16 reticulate) (Fig. 1*G*). This notion was also supported by hierarchical clustering analysis, which shows that the expression profiles of α-keratin genes are clustered mainly by developmental stages for all samples (Fig. S3*B*), whereas the expression profiles of feather-β-keratin genes are separate from all other samples regardless of developmental stages (Fig. 1*H*). We also observed that feathers have a higher proportion of differentially expressed β-keratin genes than other keratinized structures

Table 1. Number of differentially expressed keratin genes among different skin appendages at E14

Embryonic age and skin appendage type	E14 Feather	E14 Scutate	E14 Reticulate	E14 Claw	E14 Beak
E14 Feather		85 (85%)	90 (90%)	87 (87%)	94 (94%)
E14 Scutate	14 (70%)		12 (12%)	39 (39%)	33 (33%)
E14 Reticulate	14 (70%)	7 (35%)		40 (40%)	33 (33%)
E14 Claw	10 (50%)	13 (65%)	15 (75%)		35 (35%)
E14 Beak	13 (65%)	14 (70%)	17 (85%)	15 (75%)	

The numbers are obtained by RNA-seq analysis and individual paralogs were identified by their UTR and coding sequences. Below the diagonal, α-keratins; above the diagonal, β-keratins. The number refers to the number of differentially expressed keratin genes. The number in parentheses represents the percentage of total α- or β-keratin genes.

(Table 1). In contrast, α-keratin genes did not show this difference. This observation suggests that β-keratin expression patterns are responsible for the characteristics of these keratinized skin appendages, whereas α-keratins may provide important platforms or scaffolds upon which these structures develop.

We found that embryonic feathers mainly use feather-β-keratin genes from Chr1 and Chr25. Some genes from Chr27 are also used (Fig. 1*H*). The feather-β-keratin genes from Chr2 and Chr6 are only expressed in low quantities. In view of our previous study (25), feather-β-keratin genes on Chr2 and Chr6 are likely to be expressed in the rachis of body and flight feathers, but are absent in downy feathers. The only feather-β-keratin gene on Chr7 is expressed in the ramus of contour and flight feathers but weakly expressed in downy feathers. These data suggest that feather-β-keratin genes on different chromosomes may encode for different β-keratin proteins that have specific biochemical and biophysical properties to make distinct types of feather structures. These observations also indicate that feather-β-keratin gene expansion and divergence on different chromosomes were critical for the evolution of feather types and functions.

In Situ Hybridization of Specific α-Keratin Probes. To verify the differential expression of keratin genes revealed by RNA-seq, we performed SISH by using specific probes. α-keratins include type I (acidic) and type II (basic/neutral) clusters, which have 16 and 18 genes located in Chr27 and ChrLGE22C19W28_E50C23, respectively. One member each from types I and II form a specific keratin pair (25). The probes were designed from the 3′ UTR (untranslated region) of mRNA (Table S2). *KRT13A* and *KRT75A*, respectively, were chosen as representatives of type I and type II α-keratin genes that are expressed at a higher level in the feathers than in other skin appendages. *KRT14* and *KRT5* were used as representatives of type I and type II α-keratin genes that are expressed at similar levels in feathers as in other skin appendages.

To ensure that the SISH results were not affected by artifacts produced by independent sample handling, different samples of the same embryonic stage were fixed as a group and embedded within the same paraffin block to perform SISH. The expression patterns at E16 are shown in Fig. 2. The data from both E14 and E16 are shown in Fig. S4.

SISH detected the presence of *KRT13A* transcripts in both the upper and lower beak (Fig. 2*A* and Fig. S4*A*). *KRT13A* was expressed in the feather sheath and barb ridge at E14 and E16 (Fig. 2*A* and Fig. S4*A*). In the scutate scales, *KRT13A* transcripts were not detected at E14 but became predominantly expressed in the outer surface at E16 (Fig. 2*A* and Fig. S4*A*). In reticulate scales, *KRT13A* appeared faintly in periderm at both stages (Fig. 2*A* and Fig. S4*A*). At both E14 and E16, *KRT13A* transcripts were detected in the claw in both the unguis and subunguis (Fig. 2*A* and Fig. S4*A*). In all skin appendages that were positive for *KRT13A*, the transcripts were absent in the basal layer. In comparison, another type I keratin gene, *KRT14*, was expressed in the basal layer with a similar pattern in all different skin appendages (Fig. 2*B* and Fig. S4*B*).

The type II α-keratin gene *KRT75A* was detected in the stratum intermedium of both the upper and lower beak at E14 and E16 (Fig. 2*C* and Fig. S4*C*). *KRT75A* expression was detected in the feather ramus region at both E14 and E16 (Fig. 2*C* and Fig. S4*C*). The patterns match those reported in Ng et al. that were generated by using a probe from the coding region (25). *KRT75A* transcripts were detected in the subperiderm of both the outer surface and hinge regions of scutate scales at E14 and E16 (Fig. 2*C* and Fig. S4*C*). The subperiderm layer of reticulate scale

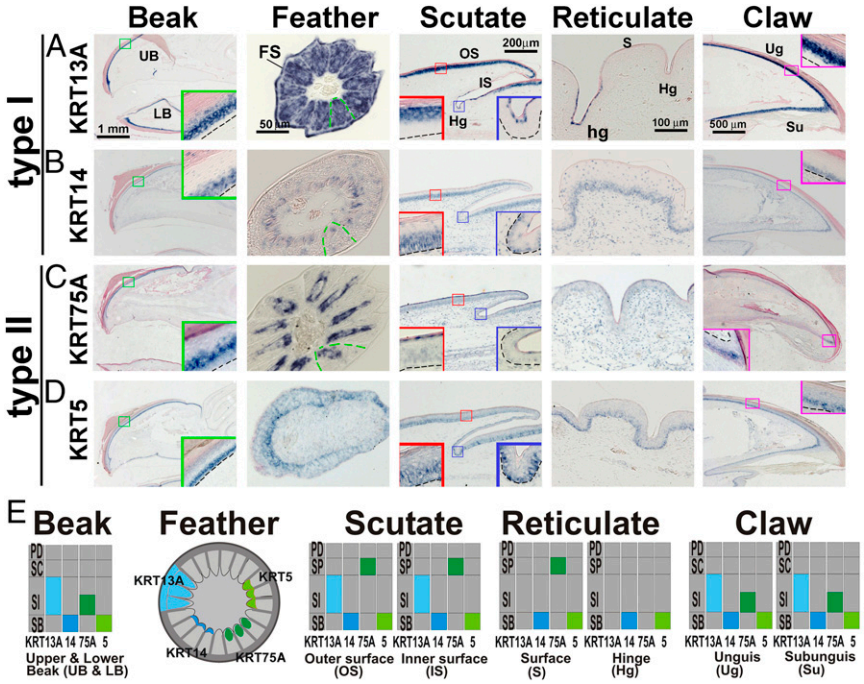

Fig. 2. In situ hybridization of α-keratin transcripts in different skin appendages at E16. Type I α-keratin genes KRT13A (*A*) and KRT14 (*B*). Type II α-keratin genes KRT75A (*C*) and KRT5 (*D*). *Insets* in *A*–*D* are higher magnification views of the indicated area. Black dotted line indicates the basement membrane. Green dotted line indicates the barb ridge. (*E*) Summary of expression of four α-keratin genes in different skin appendages. In the same feather cross-section, we used three barb ridges to present the expression of each α-keratin. To demonstrate the spatial difference in other skin appendages, we distinguished between the scutate scale outer surface and the inner surface, between the reticulate scale surface and hinge, and between the claw unguis and subunguis. Colored blocks indicate the positive epidermis layer. Light blue, KRT13; blue, KRT14; green, KRT75A; light green, KRT5. Et; egg tooth; FS, feather sheath; Hg, hinge; IS, inner surface; LB, lower beak, OS, outer surface; PD, periderm; S, surface; SB, stratum basal; SC, stratum corneum; SI, stratum intermedium; SP, subperiderm; Su, subunguis; UB; upper beak, Ug, unguis.

surface stains faintly positive for *KRT75A* (Fig. 2*C* and Fig. S4*C*). In the claw, *KRT75A* was detected in the stratum intermedium at E14 and E16, but higher levels were detected in the subunguis at both stages (Fig. 2*C* and Fig. S4*C*). In comparison, *KRT5* transcripts were detected in the basal layer of most skin appendages (Fig. 2*D* and Fig. S4*D*). The expression patterns of these four α-keratins are summarized in Fig. 2*E*. The α-keratin SISH data demonstrated the differential expression of α-keratin in different developing skin appendages, suggesting that temporal and spatial α-keratin expression may be involved in establishing the diversity of skin appendage phenotypes during their morphogenesis (38).

In Situ Hybridization of Selective Specific β-Keratin Probes. RNA-seq data demonstrated that β-keratin genes in Chr25 are differentially expressed in different skin appendages. There are four main clusters of β-keratin genes in Chr25, including claw keratin, feather keratin, scale keratin, and keratinocyte keratin (14, 25). We performed SISH on one representative for each group. The probes used were from the genes coding for claw-β-keratin 9 (Claw9), feather-β-keratin 12 (FK12), scale-β-keratin 18 (Scale18), and keratinocyte-β-keratin 13 (Ktn13) (Table S2). The expression patterns at E16 are shown in Fig. 3. The data from both E14 and E16 are shown in Fig. S5.

Claw9 transcripts were detected in the outer-oral epidermis in the E14 and E16 beak (Fig. 3*A* and Fig. S5*A*). *Claw9* was not detected in feather and reticulate scales at E14 or E16 (Fig. 3*A* and Fig. S5*A*). In scutate scales, *Claw9* was not detected at E14 but was strongly expressed in the periderm and weakly expressed in the subperiderm of the outer surface at E16 (Fig. 3*A* and Fig. S5*A*). In claws at both E14 and E16, *Claw9* was detected in the unguis but not in the subunguis (Fig. 3*A* and Fig. S5*A*).

FK12 was detected in the barb ridge of E14 and E16 feather filament (Fig. 3*B* and Fig. S5*B*). In scutate scales, *FK12* was absent at E14 but present in the periderm of the outer surface at E16 (Fig. 3*B* and Fig. S5*B*). In other skin appendages, including beaks, reticulate scales, and claws, *FK12* was not detected at E14 nor E16 (Fig. 3*B* and Fig. S5*B*).

Scale18 was expressed in the upper and lower beak (Fig. 3*C* and Fig. S5*C*). *Scale18* was also detected in inner-oral regions of the lower beak (Fig. S5*C*, arrow). *Scale18* was absent in feathers and reticulate scales (Fig. 3*C* and Fig. S5*C*). In scutate scales, *Scale18* was detected in the subperiderm and stratum intermedium of the outer surface at both E14 and E16 (Fig. 3*C* and Fig. S5*C*). Scale18 transcripts were also faintly detected in the stratum intermedium layer of the unguis and outer-oral regions of the claw (Fig. 3*C* and Fig. S5*C*).

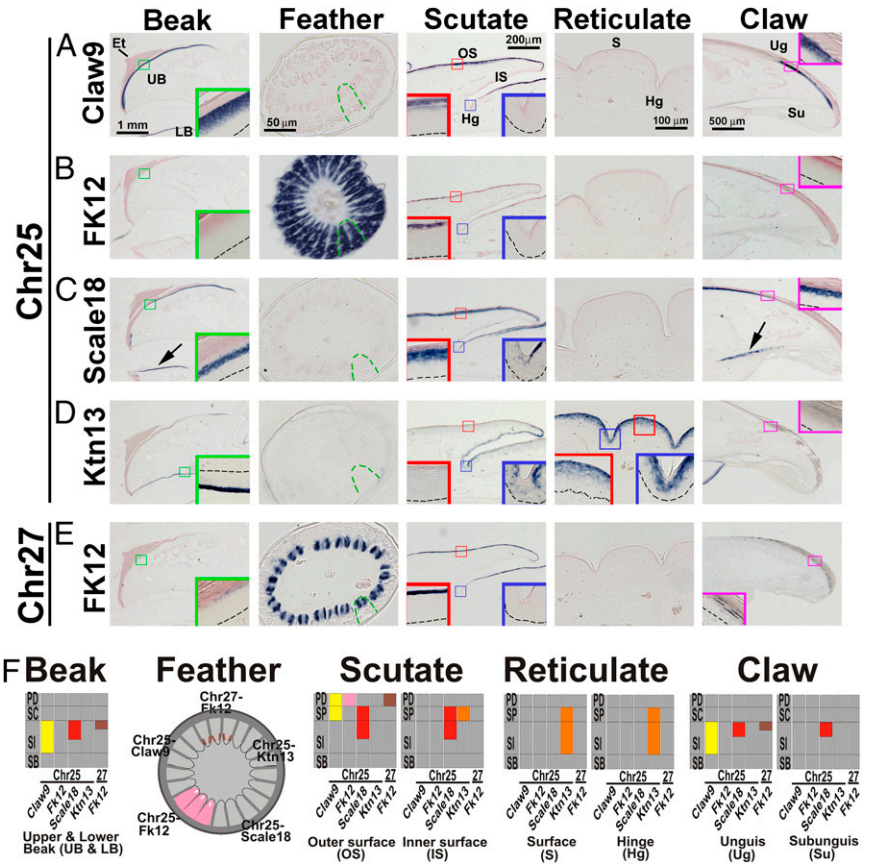

Fig. 3. In situ hybridization of five β-keratin transcripts encoded on Chr25 and Chr27 in different skin appendages at E16. (*A*) Chr25-Claw9. (*B*) Chr25-FK12. (*C*) Chr25-Scale18. (*D*) Chr25-Ktn13. Chr27-FK12 (*E*). *Insets* in *A*–*E* are higher magnification views of the indicated area. Arrows in *C* indicate the expression of the Scale18 gene in the lower beak inner-oral epidermis and subunguis. Black dotted line indicates the basement membrane. Green dotted line indicates the barb ridge. (*F*) Summary of the expression patterns of five β-keratin genes in different skin appendages. In the same feather cross-section, we used three barb ridges to present the expression of each β-keratin gene. To demonstrate the spatial difference in other skin appendages, we distinguished between the scutate scale outer surface and inner surface, between the reticulate scale surface and hinge, and between the claw unguis and subunguis. Colored blocks indicate the positive epidermis layer. Yellow, Chr25-Claw9; pink, Chr25-FK12; red, Chr25-Scale18; orange, Chr25-Ktn13; brown, Chr27-Fk12. Et; egg tooth; FS, feather sheath; Hg, hinge; IS, inner surface; LB, lower beak, OS, outer surface; PD, periderm; S, surface; SB, stratum basal; SC, stratum corneum; SI, stratum intermedium; SP, subperiderm; Su, subunguis; UB; upper beak, Ug, unguis.

Among skin appendages, *Ktn13* transcripts was detected in the tip of the beak at E14 and the inner-oral epidermis of upper beak at E16 (Fig. 3*D* and Fig. S5*D*). *Ktn13* were also detected at E16 in the subperiderm of scutate scale's inner surface and the hinge region (Fig. 3*D* and Fig. S5*D*) and the subperiderm and stratum intermedium layers of the reticulate scale (Fig. 3*D* and Fig. S5*D*). *Ktn13* was not detected in the feather or claw (Fig. 3*D* and Fig. S5*D*).

There are 63 annotated feather keratins distributed along chromosome 27 (25). We wondered whether these feather keratins have similar expression patterns as the feather-β-keratins encoded on chromosome 25. We generated a feather-β-keratin gene probe from chromosome 27 (*Chr27-FK12*; Table S2). In the feather filament, *Chr27-FK12* showed a distinct expression pattern in the barb cortical region (Fig. 3*E* and Fig. S5*E*). This pattern is distinguished from that of *Chr25-FK12*, which showed expression in the barbule plate (Fig. 3*B*). In scutate scales, *Chr27-FK12* was strongly expressed in the E16 outer surface periderm (Fig. 3*E* and Fig. S5*E*). *Chr27-FK12* was also faintly expressed in the beak and claw stratum intermedium close to the stratum corneum (Fig. 3*E* and Fig. S5*E*). The expression patterns of these five β-keratins are summarized in Fig. 3*F*.

The β-keratin SISH data demonstrated the differential expression of β-keratin genes in different developing skin appendages. Together, the α- and β-keratin SISH data suggest that temporal and spatial expression of both α- and β-keratin genes may affect the properties of different skin appendages, producing different structural phenotypes. Keratinocytes residing in different skin appendages and even within the same appendage may express different amounts of α- and β-keratin genes, leading to expanded skin appendage diversity.

Effects of *KRT5* Mutant Forms on Feather Formation. In our previous work studying the role of α-keratins in feather morphogenesis, we ectopically expressed three *KRT5* mutant forms mimicking the mutant forms seen in a rare human skin disease, by deleting, respectively, Asn183 (mt1), Val170_Lys191 (mt2), and Arg464_Ala468 (mt3) of chicken *KRT5* (25). These mutations in chicken *KRT5* correspond to Asn177, Val-164_Lys-185, and Arg429_Ala433 of human K5, which are associated with the Dowling-Meara type of epidermolysis bullosa herpetiformis (39–41). Adult feather follicles were injected with RCAS virus directing the expression of mutant *KRT5*. Ensuing changes in branching morphogenesis and growth defects were observed (25). Here, we tested the effects of overexpressing mutant cDNAs on embryonic skin appendage development.

The three mutant forms all showed an abnormal feather filament. The abnormal phenotype from mutant form 3 is shown in Fig. 4*B* (arrows). When RCAS-GFP was used as a control, no phenotypic change was observed in either whole-mount bright field view or in paraffin sections (Fig. 4 *A* and *D*). Comparing H&E staining from sections of the GFP control and mutant form revealed that *KRT5* mutations induce alterations in barb ridge formation (Fig. 4*E*, compared with Fig. 4*D*). Each of these mutations led to an enlarged ramus forming area with larger medullary cells (red arrows in Fig. 4*E*). In situ hybridization using a common β-keratin probe (Fig. 4*H*) showed that β-keratin is expressed around the enlarged medullary cells with a reduced domain size (green arrows, Fig. 4*H*), compared with the control (Fig. 4*G*). In situ hybridization using a common type-II α-keratin probe showed that type-II α-keratin is only present surrounding but not in the medullary cells (purple arrows, Fig. 4*K*, compared with the control in Fig. 4*J*). Confocal microscopy of β-keratin (green color) and KRT75 (red color) showed not only the reduced β-keratin positive area in the barbule cells but also the complex KRT75 network in medullary cells (Fig. 4*N*, compared with the control in Fig. 4*M*). The data indicate that the *KRT5* mutation not only affects the expression of other α-keratin genes but also the distribution of β-keratin transcripts.

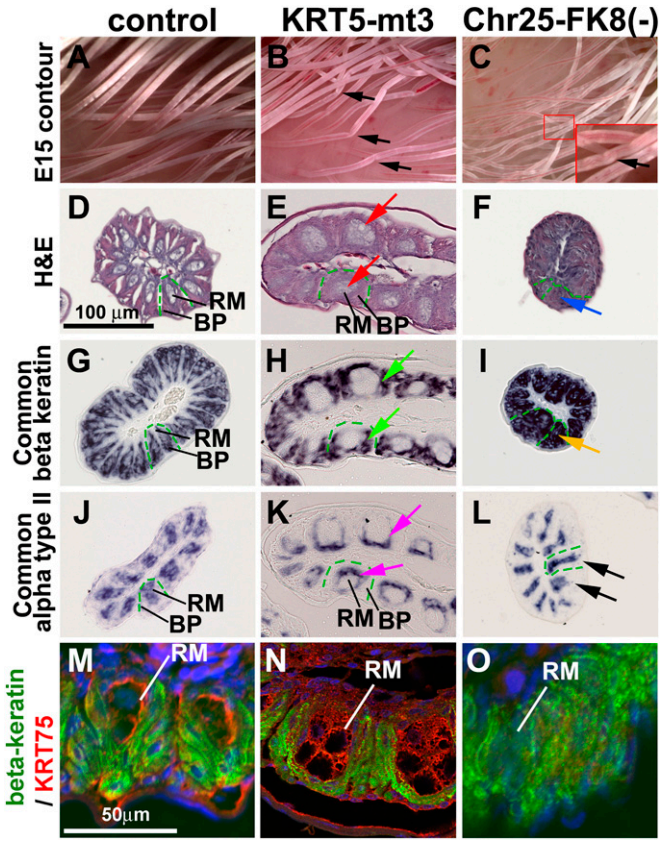

Fig. 4. Functional study shown by overexpressing α-keratins KRT5 mutant and feather β-keratin antisense form in embryonic feather development. The interdependence of α- and β-keratins in forming proper keratin network is shown by functional perturbation experiment during feather regeneration. (*A–C*) Bright field view of feather filament at E15. Black arrow indicates abnormal development. (*D–F*) H&E staining of cross-sections. Red arrow indicates the enlarged ramus. Blue arrow indicates the abnormal barb ridge without clear ramus. (*G–L*) SISH. (*G–I*) Common β-keratin staining. Green arrow indicates the β-keratin expression domain surrounding the enlarged ramus. Yellow arrow indicates the smaller β-keratin negative domain. (*J–L*) Common type-II α-keratin staining. Purple arrow indicates the expression of type II α-keratin, which surrounds the enlarged ramus. Black arrow indicates the abnormal expression of type II α-keratin. Dotted green lines indicate a barb ridge. (*M–O*) Confocal microscopy of double staining for β-keratin (green) and KRT75 (red). (*A, D, G, J,* and *M*) RCAS-GFP control. (*B, E, H, K,* and *N*) KRT5 mutant form 3. (*C, F, I, L,* and *O*) Feather keratin 8 antisense form. BP, barb plate; RM, ramus.

Effects of β-Keratin Antisense RNA on Keratin Network Organization. To study the role of β-keratins in the keratin network and feather morphogenesis, we constructed RCAS retroviral vectors directing the synthesis of antisense β-keratin RNAs to suppress endogenous β-keratin expression. Two constructs, Chr25-FK5 (FK5(-)) and Chr25-FK8 (FK8(-)), were prepared. Injecting the RCAS virus transcribing antisense RNA against either feather keratin form caused similar abnormal feather filament formation. FK8(-)-infected feathers were much thinner than the RCAS-GFP control (compare Fig. 4*C* to Fig. 4*A*). FK8(-)-infected feathers also showed abnormal feather filaments with a twisted morphology (arrow in Fig. 4*C*). H&E staining showed that the barb ridges are irregular and the number of medullary cells decreased (Fig. 4*F*, blue arrow). Further examination by in situ hybridization using common β-keratin probes showed that there is a smaller β-keratin negative domain in the ramus forming area (yellow arrow, Fig. 4*I*). The type-II α-keratin expression domain became irregular in size and shape (black arrows in Fig. 4*L*, compared with Fig. 4*J*). Confocal microscopy of β-keratin

(green color) and KRT75 (red color) showed no discernable KRT75-positive medullary cells. The β-keratin domain was also arranged in an irregular pattern (Fig. 4*O*). Thus, antisense mediated suppression of β-keratin genes during feather development can affect the expression of both α- and β-keratins and their possible interactions, leading to changes in skin appendage morphology.

Taken together, the above two functional studies showed that α- and β-keratin mutations or abnormal forms can cause defects of keratinocytes and alter feather shape. Therefore, we surmise that the interaction of α- and β-keratins is essential for skin appendage morphogenesis.

Discussion

Involvement of α- and β-Keratins in Cornification of Chicken Skin Appendages. Keratins play an important role in maintaining the cytoarchitecture of an epithelial cell. In the skin, they can be converted into a keratinized horny material such as hair, nails, or feathers in different vertebrates. This process, called cornification, occurs through the association of keratin filament proteins with keratin-associated proteins (11). In vertebrates, α-keratins are the major component for conversion of squamous epithelial cells into keratinized structures. In reptiles and birds, in addition to α-keratins, their keratinocytes express β-keratins. Thus, avian skin appendages are mainly formed from the products of α- and β-keratins (42, 43). Although the acquisition of new β-keratin genes and divergence of avian α-keratin genes most likely correlate with functional diversification, little progress has been made to characterize their specific expression profiles in different skin appendages.

α- and β-keratins have been characterized by biochemical and immunocytochemical analyses (1, 44). In birds, α-keratins (intermediate filament proteins) produce α-X-ray patterns that are present in various skin appendages (1). In chickens, five β-keratin subfamilies (claw, feather, feather-like, keratinocyte, and scale) have been classified by sequence heterogeneity and tissue-specific expression (14, 24, 25, 45–47). Each of these studies only provided rough profiles due to the limitations of older techniques. Despite their limitations, these studies demonstrated regional specificity of corneous genes in different skin appendages. The differences come in two hierarchical levels: one is different compositions of keratins in different skin appendages at the macrolevel of body regions, the other is different keratins expressed in the microlevel of detail differences within one appendage. For example, feathers and scales might use different β-keratins, whereas different parts of scutate scales (outer surface versus inner surface) might use different α- and β-keratins. At hatching, reticulate scales express three α-keratin polypeptides compared with six in scutate scales. In contrast, no β-keratins were found previously in reticulate scales (1). Further, we now found β-keratins expressed in complex ways in different parts of a feather.

Avian β-keratins have a molecular mass of 10–30 kDa, like many mammalian keratin-associated proteins (KAPs) that form an amorphous matrix around α-keratins or may replace most α-keratins to form a dense corneous material (11). Alkaline (basic) avian β-keratins interact with acidic α-keratins. This interaction is indicated by the colocalization of α- and β-keratins in scales, claws, and feathers determined by ultrastructural studies (48).

Advances in the Genomic Sequence of α- and β-Keratins Enhance Our Ability To Characterize Their Differential Expression in Skin Appendages. Recent advances in large-scale sequencing of avian genomes (13, 49) facilitate the study of α- and β-keratin gene regulation during skin appendage morphogenesis. However, mapping the β-keratin genes onto the avian genome has been challenging because of the high homology between duplicated genes. Previous genome-wide comparative analyses in zebra finches and chickens identified several β-keratin gene clusters; the largest two are on chromosomes 25 (Chr25) and 27 (Chr27) (24). Recently, we made an exhaustive search of α- and β-keratin genes in the current chicken genome assembly (Galgal4) and updated the keratin gene annotation (25).

Our α- and β-keratin gene annotation provides a higher resolution gene sequence and localization within the genome than was available previously (25). This enhanced sequence enabled us to investigate differential α- and β-keratin gene expression in various feather forms at different regeneration time points. Knowledge of the timing and tissue expression of the many α- and β-keratin genes allows us to associate feather shape with the specific α- and β-keratins produced to form the ramus, rachis, and calamus in various feather types (plumulaceous versus pennaceous, contour versus flight feathers) (25). The expression profiles of these α- and β-keratins are critical to understanding the molecular mechanism underlying the structural variation of feather diversity (38).

In the current study, we examined the differential expression of α- and β-keratin genes in different developing skin appendages at the genome level. Using transcriptomic analysis and specific α- and β-keratin probes, we studied their transcript distribution in embryonic feather follicles. SISH and RNA-seq showed that α- and β-keratins are preferentially expressed in different parts of skin appendages, but β-keratin genes show a higher level of differential expression (Fig. 5 *A* and *B*). Interestingly, feathers have a higher proportion of differentially expressed β-keratin genes compared with other skin appendages (Table 1). Embryonic chicken feathers highly use feather-β-keratin genes from Chr1, Chr10, Chr25, and some members from Chr27 in the keratinization process, whereas feather-β-keratin genes from Chr2 and Chr6 are mainly expressed in the rachis of adult contour feathers (25). This observation implies that feather keratin cluster expansion and subfunctionalization are important for avian feather evolution and diversification.

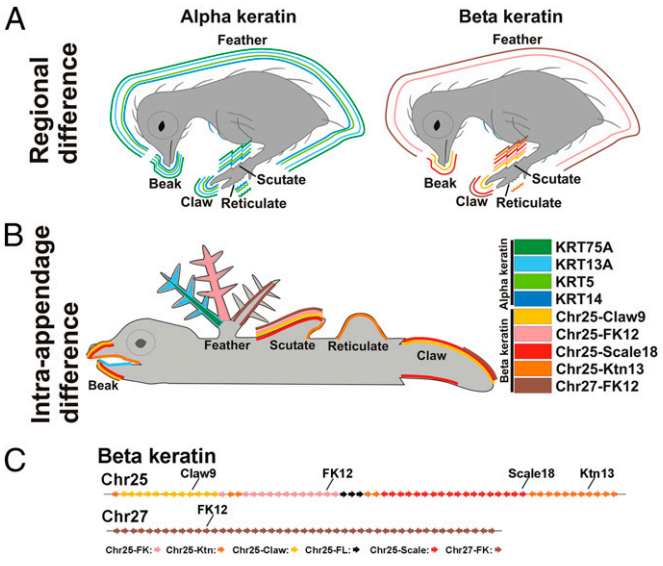

Fig. 5. Summary of topographic expression patterns of α- and β-keratin genes in different skin appendages. (*A*) Regional differences among different skin appendages. Each line indicates the expression of keratin genes in certain appendages. The missing line indicates the negative or undetectable RNA expression. (*B*) Intraappendage differences of keratin expression. We only show the differentially expressed keratin genes in *B*. Colors represent the indicated keratin genes. (*C*) β-keratin gene arrangements on Chr25 and Chr27. The marked genes are used in β-keratin in situ hybridization. Claw, claw keratin; FK, feather keratin; FL, feather-like keratin; Ktn, keratinocyte keratin; Scale, scale keratin.

It is worth mentioning that specific SISH probes for β-keratins are difficult to choose, even when using the 3′ UTR regions, especially within the same gene cluster. For example, most 3′ UTR of Chr27-Feather keratin genes are too similar to use SISH to distinguish their individual expression patterns.

Interactions of α/β-Keratins and the Assembly of Keratin Networks. To evaluate the importance of α- and β-keratin interdependence in forming keratin networks in avian keratinocytes, we performed functional analyses by using α-keratin mutant forms and β-keratin antisense forms. Each experimental condition led to the formation of abnormal feather filaments and defects in both α- and β-keratin deposition. Our data revealed that proper interactions between α- and β-keratins are critical for skin appendage morphogenesis.

Previously, we showed that mutations in *KRT75*(*KRT75A*), an α-keratin, caused a curvature of the rachis producing the Frizzle phenotype in domestic chickens (50). *KRT75* is expressed in the medulla of the rachis and ramus. In contrast, *KRT5* is expressed in the basal layer in both embryonic and adult feathers. Ectopic expression of a mutant KRT75 mimicked the Frizzle phenotype, whereas ectopic expression of a mutant *KRT5* can affect the morphogenesis of adult wing feathers. One KRT5 mutant form even caused the feathers to stop growing, which suggests that KRT5 can affect keratinocyte fate and behavior (25). These results suggest that the distribution of α-keratin expression is related to their contribution to feather shape. In the current study, we further show that expressing mutant KRT5 forms in developing feather follicles can affect embryonic feather filament morphogenesis and increase the size of the ramus while decreasing the size of feather branches (Fig. 4*E*).

The interaction between α- and β-keratins appears to be important for avian skin appendage morphogenesis. In the chicken tongue, immune-electron microscopy demonstrated that α- and β-keratins colocalize in the stratum intermedium and stratum corneum (10) and appear to be important for avian skin appendage morphogenesis. Their colocalization in filament bundles suggests that there is an as-yet-unknown functional relationship between α- and β-keratins. A recent immunocytochemical study using double-labeling immunogold showed embryonic feather barb and barbule cells are full of small feather-β-proteins. These feather-β-proteins may form compact corneous materials in barb and barbule cells (11). There may be direct interactions between α-keratin filaments and β-keratin filaments that maintains homeostasis among α- and β-keratins within cells. Furthermore, the stoichometry among α- and β-keratins could vary in different feather epithelia. The fact that changes of either keratin type can lead to a disrupted keratin network and cause perturbed expression at both mRNA and protein levels suggests their intimate relationship. However, it is still unknown whether such feedback dependence acts at the transcriptional or translational level.

The current study helps us understand how a complex structure has evolved by reconstructing new cytoskeletal networks. Suppressing the expression of a β-keratin genes altered the expression of α-keratin at both mRNA and protein levels. Although avian and reptilian β-keratins can form long fibrous polymers that differ completely from those of α-keratins, these data suggest that β-keratins may also feedback to regulate α-keratin expression. Based on ultrastructural studies, 8- to 10-nm α-keratin filaments formed and then were replaced or masked by 3- to 4-nm-thick β-keratin filaments (48), suggesting that the normal spatial and temporal expression of α-keratin is required for the proper formation of β-keratin filaments.

Besides for being structural proteins, α-keratins are also increasingly recognized as regulators of other cellular properties and functions, including apico-basal polarization, cell motility, cell size, cell transport, cell compartmentalization, cell differentiation, protein synthesis, membrane trafficking, and signaling (51–58). Many diseases associated with mutations in α-keratin genes may not be due to structural alterations, but rather involvement in organizing cytoplasmic architecture, signaling, and/or regulating transcription (59). Suppressing β-keratin genes significantly affects the expression of α-keratin genes, suggesting that β-keratins may also have nonstructural and mechanical functions as well. However, whether β-keratins directly participate in other cellular functions or affect the expression of α-keratin genes via disruption of intermediate filament networks are worth investigating in the future.

Our results using a molecular approach demonstrate that expression and interactions of α- and β-keratins are critical for keratinization and are essential for appropriate feather morphogenesis during development. Combined, these data suggest that α-keratin gene coding sequences and their cis-regulatory elements evolved to participate in protein–protein interactions and regulatory networks controlling the cornification of skin appendages in avians. Our current study helps us understand how a complex structure evolved by constructing new cytoskeletal networks.

The expression and functional data suggest that each keratinocyte in different skin appendages and within the same appendage may express different amounts of α- and β-keratin components. Mutations in α- or β-keratins or an antisense form can cause defective keratin deposition and alter the morphogenesis process. The differential combination of keratin types (hard/soft, flexible/rigid) may alter skin appendage properties and offer novel functions. Specific α- or β-keratin expression in skin appendage subdomains may fine tune skin appendage structure and function. These refined expression patterns would enable the development of diverse skin appendage forms to open new environmental niches for evolutionary selection.

Evolutionary Perspective on how Cytoskeletal Network Evolution Expanded Architectural Features in Skin Appendages. Avian genomes may be more static compared with mammalian genomes (60). Despite their highly innovative morphological features, few unique changes have been detected in different bird genomes. Evolutionarily novel genes associated with feather development were largely unknown. The radiation and expansion of β-keratins are among the few obvious changes found on the lineage leading to birds (14, 24, 26, 61). The emergence of novel, lineage-specific, morphological features is known to have occurred through gene family expansions (62). Our RNA-seq data showed that embryonic chicken feathers mainly use feather-β-keratin genes from Chr1, Chr10, Chr25, and some of feather-β-keratin genes from Chr27 during the keratinization process. This finding indicates that at least 74.5% of total β-keratin genes are involved, implying that feather keratin cluster expansion was important for the diversification of chicken feathers, although the function of β-keratins has not been studied until now. Given the fact that β-keratins are expressed in novel substructures of feather rachis and barbs, it would be particularly interesting to study the regulatory regions of these keratins. A comparative genomic study was taken to identify conserved nonexonic regulatory elements in the genomes of archosaur lineage, but no exceptional expansion was identified near avian β-keratins (12). We are using ChIP-seq analyses to identify the regulatory elements of the keratin complexes. It will be exciting to see whether future studies in the field find that the regulatory elements reside beside each α- or β-keratin gene or if there is a master regulatory element located outside of the whole cluster.

The sauropsid ancestor evolved fibrous β-keratins that contain mostly β-pleated sheets and form fibrous polymers and filaments instead of an amorphous matrix as occurs with mammalian KAPs (11). There is no evidence of mammalian KAP proteins in fishes or amphibians, suggesting that mammalian KAPs and reptilian β-keratins are not homologous. Differences in the KAP gene

repertoire, gene expression, and molecular evolution were suggested to be responsible for microphenotypic and macrophenotypic hair diversification among mammals in response to adaptations to ecological pressures. A smaller type of fibrous β-keratins, identified as feather-β-keratins, permits the formation of branched barbs and feathers and evolved in the lineage of archosaurian reptiles from which birds are derived (15, 20, 63). Feather-β-keratins are prevalently organized along parallel fibers, whereas scale- or claw-β-keratins have a more irregular orientation and interwoven structure, making feathers more flexible but less resistant to abrasion (11). The arrangement of the β-keratins in the cortex (outer shell) and medulla (central foam-like configuration) add physical strength to the feather structure although the precise details underlying this domain-specific expression still are unknown (64).

Birds have scales on their feet. Because avian scales seem to resemble reptilian scales and are also composed mainly of β-keratins, some scholars have proposed that they are homologous. Alternatively, the overlapping scales of birds have been proposed to develop later in evolution, being secondarily derived (34, 35). Given the evidence of the four winged feathered dinosaurs (63), birds might have originally been entirely covered by feathers, except for the plantar surface of their feet, in which the feather formation program is blocked at its initiation step. Studies on the avian embryonic cell lineage of feathers and scales and the reptilian lineage of scales suggest that these processes are homologous (34–36). These processes probably use conserved signaling modules in their common ancestors (34), but then modify the signaling modules to form different mature appendage phenotypes. Further comparisons of signaling molecules and structural protein analyses such as keratins should enhance the understanding of skin appendage evolution in the future.

In summary, by exploring α- and β-keratin gene expression in different skin appendages, our findings extend research on embryonic skin appendages. RNA-seq data showed that β-keratin genes have a distinct expression profile in each skin appendage (Fig. 2*G*). Five representative β-keratin gene clusters on chromosomes 25 and 27 showed expression specificity among different appendages and even within the same appendage (Figs. 3*F* and 5 *A*–*C*). For example, feather-β-keratins on chromosome 25 and 27 have distinct expression patterns in the barb ridge (Fig. 3*F*). The former (*Chr25-FK12*) is expressed in the barb plate (the future barbules), whereas the latter (*Chr27-FK12*) is in the cortical cells of the ramus. This result suggests that β-keratin paralogs on different chromosomes may play different roles during feather morphogenesis and may be under different regulation. Insights from this study highlight the importance of α- and β-keratins to the structure and function of ectodermal organs, which contribute to the origin and evolution of feathers. Further studies will be necessary to illustrate the temporal and spatial control of keratin gene cluster regulation. Overall, our data suggest that morphological and structural diversity of skin appendages can largely be attributed to the differential combinations of α- and β-keratin genes; both α- and β-keratin are required for the proper assembly of keratin network in chicken keratinocytes. Moreover, β-keratins play a more important role in producing elaborate feather architectures. How α- and β-keratins are induced at the right time and space to build novel and complex skin appendages in development and evolution will be the next challenge.

Materials and Methods

Eggs. Pathogen-free fertilized eggs were purchased from SPAFAS. For viral-mediated functional studies, 4 μL of concentrated RCAS viruses was injected to the amniotic cavity at E3 (stage 18) and samples were collected at E15 (stage 41).

Construction of RCAS-KRT5 Mutant Forms. The three KRT5 mutant forms were cloned as described in Ng et al. (25). KRT5-N183Δ, KRT5-R464_A468Δ, and KRT5-V170_K191Δ were generated by using the QuikChange Lightening Site-Directed Mutagenesis Kit (Agilent Technologies) and the QuikChange Lightening Multi Site-Directed Mutagenesis Kit (Agilent Technologies). Mutated genes were transferred to the cDNAs to a Gateway compatible RCASBP-Y DV vector. Virus was made according to Jiang et al. and concentrated by ultracentrifugation (65).

Construction of RCAS-β-Keratin Antisense Form. To construct the β-keratin antisense form, we used RT-PCR to clone feather keratin 5 (FK5) and 8 (FK8) genes, which both reside on Chr25. PCR primers, FK5-forward, (5′-CTCTCCA-GGTCCACCTCCAT-3′), Fk5-backward (5′-TTCCCGGGCTATAACATCTG-3′); and FK8-forward, (5′-GGTGAAAAAGTCCACCTCCA-3′), FK8-backward, (5′-TTCTTT-GCAGGACAGAGCAA-3′). The PCR products were then cloned into RCAS in the antisense orientation and validated by sequencing.

RNA-seq. RNA-seq was performed on replicate samples from E14 embryos (feathers, scutate scales, reticulate scales, claws, and beaks) and E16 embryos (scutate scales, reticulate scales; Table S1). For all embryonic samples, RNA was extracted by using TRIzol reagent (Invitrogen) from combined epidermis and dermis. Two micrograms of total RNA from each sample was used to construct an RNA-seq library by using TruSeq RNA sample preparation v2 kit (Illumina). Sequencing (50 cycles single read) was performed by using Hi-seq 2000 at the University of Southern California Epigenome Center. RNA-seq mapping was done as described (25).

Read Mapping and Transcriptome Analyses. TopHat2 was used for alignment. HTSeq software was used to count the number of reads mapped to each gene (66). If the fragments were multiply mapped on different genes, the reads will be removed from the analysis. The weighted trimmed mean of the log expression ratios (trimmed mean of M values) were calculated for normalization (67). PCA was carried out on normalized read counts by using edgeR (68). Genes differentially expressed among embryonic samples were determined by edgeR. False discovery rate <0.05 was used as a threshold to determine significant differences in gene expression. For hierarchical clustering, quantification and normalization were performed by Partek E/M and FPKM, respectively.

Paraffin Section. Chicken embryos were collected, fixed in 4% (wt/vol) paraformaldehyde at 4 °C overnight for immunohistochemistry, and 7-μm paraffin sections were prepared, following the procedures described by Jiang et al. (65). Skin appendages from the same stage were fixed as a group and embedded within the same paraffin block to ensure that different samples were prepared by using the same fixation and in situ hybridization conditions. For each stage, two sets of samples were prepared in duplicate.

mRNA in Situ Hybridization. To generate specific α- and β-keratin antisense RNA probes, we used the 3′ UTR (untranslated region) mRNA region as PCR targets. PCR primers for each keratin form are listed in Table S2. We also include a common type-II α-keratin probe and a common β-keratin probe, using the conserved coding region as the PCR target (Table S2). The PCR product was inserted into the p-drive plasmid (Qiagen). Nonradioactive in situ hybridization was performed according to procedures described in Chuong et al. (69). Diluted eosin was used for faint counterstaining.

Immunostaining and Imaging. Double fluorescent immunostaining was performed by using antibodies against human KRT75 (ab76486; Abcam) or β-keratin (a gift from Roger Sawyer, University of South Carolina, Columbia, SC). We used Alexa Fluor 546 anti-mouse IgG (A11030) and 488 anti-rabbit IgG (A11008) as secondary antibodies, respectively. Sections were imaged with a Zeiss 510 confocal microscope (University of Southern California, Liver Center). DAPI was used to visualize the nuclei.

ACKNOWLEDGMENTS. We thank the University of Southern California (USC) Epigenome Core Facility for conducting Illumina transcriptome sequencing, the University of Southern California's Norris Medical Library Bioinformatics Service for assisting with sequencing data analysis, Drs. Mei-Yeh Lu and Tzi-Tuan Wang for technical assistance, and Dr. Roger Sawyer for providing the β-keratin antibody and for his constructive suggestions during the preparation of this paper. Some of the bioinformatics software and computing resources used in the analysis are funded by the USC Office of Research and the Norris Medical Library. Research reported in this publication was supported by the National Institute of Arthritis and Musculoskeletal and Skin Diseases of the National Institutes of Health under Award Numbers AR 47364 and AR 60306; National Science Council, Taiwan Grant 99-2321-B-001-041-MY2; and Academia Sinica, Taiwan.

1. Sawyer RH, Knapp LW, O'Guin WM (1986) Epidermis, dermis and appendages. *Biology of the Integument 2 Vertebrates*, eds Bereiter-Hahn J, Matoltsy AG, Richards KS (Springer, Berlin), Vol 2, pp 194–238.
2. Chuong CM, et al. (2002) What is the 'true' function of skin? *Exp Dermatol* 11(2):159–187.
3. Chuong CM, Homberger DG (2003) Development and evolution of the amniote integument: Current landscape and future horizon. *J Exp Zoolog B Mol Dev Evol* 298(1):1–11.
4. Wu P, et al. (2004) Evo-Devo of amniote integuments and appendages. *Int J Dev Biol* 48(2-3):249–270.
5. Harris RM, Hofmann HA (2015) Seeing is believing: Dynamic evolution of gene families. *Proc Natl Acad Sci USA* 112(5):1252–1253.
6. Ohno S (1970) *Evolution by Gene Duplication* (Springer, New York).
7. Chen CF, et al. (2015) Development, regeneration, and evolution of feathers. *Annu Rev Anim Biosci* 3:169–195.
8. Yu M, et al. (2004) The biology of feather follicles. *Int J Dev Biol* 48(2–3):181–191.
9. Shames RB, Knapp LW, Carver WE, Sawyer RH (1988) Identification, expression, and localization of beta keratin gene products during development of avian scutate scales. *Differentiation* 38(2):115–123.
10. Carver WE, Sawyer RH (1989) Immunocytochemical localization and biochemical analysis of alpha and beta keratins in the avian lingual epithelium. *Am J Anat* 184(1): 66–75.
11. Alibardi L, Toni M (2008) Cytochemical and molecular characteristics of the process of cornification during feather morphogenesis. *Prog Histochem Cytochem* 43(1):1–69.
12. Lowe CB, Clarke JA, Baker AJ, Haussler D, Edwards SV (2015) Feather development genes and associated regulatory innovation predate the origin of Dinosauria. *Mol Biol Evol* 32(1):23–28.
13. Zhang G, et al.; Avian Genome Consortium (2014) Comparative genomics reveals insights into avian genome evolution and adaptation. *Science* 346(6215):1311–1320.
14. Greenwold MJ, et al. (2014) Dynamic evolution of the alpha (α) and beta (β) keratins has accompanied integument diversification and the adaptation of birds into novel lifestyles. *BMC Evol Biol* 14:249.
15. Vandebergh W, Bossuyt F (2012) Radiation and functional diversification of alpha keratins during early vertebrate evolution. *Mol Biol Evol* 29(3):995–1004.
16. Prum RO (1999) Development and evolutionary origin of feathers. *J Exp Zool* 285(4): 291–306.
17. Prum RO (2005) Evolution of the morphological innovations of feathers. *J Exp Zoolog B Mol Dev Evol* 304(6):570–579.
18. Prum RO, Brush AH (2002) The evolutionary origin and diversification of feathers. *Q Rev Biol* 77(3):261–295.
19. Xu X, et al. (2014) An integrative approach to understanding bird origins. *Science* 346(6215):1253293.
20. Yue Z, Jiang TX, Widelitz RB, Chuong CM (2006) Wnt3a gradient converts radial to bilateral feather symmetry via topological arrangement of epithelia. *Proc Natl Acad Sci USA* 103(4):951–955.
21. Jiang TX, Tuan TL, Wu P, Widelitz RB, Chuong CM (2011) From buds to follicles: Matrix metalloproteinases in developmental tissue remodeling during feather morphogenesis. *Differentiation* 81(5):307–314.
22. Yue Z, Jiang TX, Widelitz RB, Chuong CM (2005) Mapping stem cell activities in the feather follicle. *Nature* 438(7070):1026–1029.
23. Chuong CM, Bhat R, Widelitz RB, Bissell MJ (2014) SnapShot: Branching morphogenesis. *Cell* 158(5):1212–1212.e1.
24. Greenwold MJ, Sawyer RH (2010) Genomic organization and molecular phylogenies of the beta (beta) keratin multigene family in the chicken (Gallus gallus) and zebra finch (Taeniopygia guttata): Implications for feather evolution. *BMC Evol Biol* 10:148.
25. Ng CS, et al. (2014) Genomic organization, transcriptomic analysis, and functional characterization of avian α- and β-keratins in diverse feather forms. *Genome Biol Evol* 6(9):2258–2273.
26. Greenwold MJ, Sawyer RH (2013) Molecular evolution and expression of archosaurian β-keratins: Diversification and expansion of archosaurian β-keratins and the origin of feather β-keratins. *J Exp Zoolog B Mol Dev Evol* 320(6):393–405.
27. Greenwold MJ, Sawyer RH (2011) Linking the molecular evolution of avian beta (β) keratins to the evolution of feathers. *J Exp Zoolog B Mol Dev Evol* 316(8):609–616.
28. Chuong CM, et al. (2003) Adaptation to the sky: Defining the feather with integument fossils from mesozoic China and experimental evidence from molecular laboratories. *J Exp Zoolog B Mol Dev Evol* 298(1):42–56.
29. Kowata K, et al. (2014) Identification of a feather β-keratin gene exclusively expressed in pennaceous barbule cells of contour feathers in chicken. *Gene* 542(1):23–28.
30. Hamburger V, Hamilton HL (1951) A series of normal stages in the development of the chick embryo. *J Morphol* 88(1):49–92.
31. Lucas AM, Stettenheim PR (1972) Avian anatomy. Integument. *Agriculture Handbook 362*, (US Dept Ag, Washington, DC).
32. Sawyer RH, Abbott UK, Fry GN (1974) Avian scale development. IV. Ultrastructure of the anterior shank skin of the scaleless mutant. *J Exp Zool* 190(1):71–78.
33. Sawyer RH, Abbott UK, Fry GN (1974) Avian scale development. III. Ultrastructure of the keratinizing cells of the outer and inner epidermal surfaces of the scale ridge. *J Exp Zool* 190(1):57–70.
34. Sawyer RH, Knapp LW (2003) Avian skin development and the evolutionary origin of feathers. *J Exp Zoolog B Mol Dev Evol* 298(1):57–72.
35. Sawyer RH, Rogers L, Washington L, Glenn TC, Knapp LW (2005) Evolutionary origin of the feather epidermis. *Dev Dyn* 232(2):256–267.
36. Alibardi L, Knapp LW, Sawyer RH (2006) Beta-keratin localization in developing alligator scales and feathers in relation to the development and evolution of feathers. *J Submicrosc Cytol Pathol* 38(2-3):175–192.
37. Strasser B, Mlitz V, Hermann M, Tschachler E, Eckhart L (2015) Convergent evolution of cysteine-rich proteins in feathers and hair. *BMC Evol Biol* 15:82.
38. Rice RH, Winters BR, Durbin-Johnson BP, Rocke DM (2013) Chicken corneocyte cross-linked proteome. *J Proteome Res* 12(2):771–776.
39. Kang TW, Lee JS, Kim SE, Oh SW, Kim SC (2010) Novel and recurrent mutations in Keratin 5 and 14 in Korean patients with Epidermolysis bullosa simplex. *J Dermatol Sci* 57(2):90–94.
40. Kemp MW, et al. (2005) A novel deletion mutation in keratin 5 causing the removal of 5 amino acids and elevated mutant mRNA levels in Dowling-Meara epidermolysis bullosa simplex. *J Invest Dermatol* 124(5):1083–1085.
41. Rugg EL, et al. (1999) Donor splice site mutation in keratin 5 causes in-frame removal of 22 amino acids of H1 and 1A rod domains in Dowling-Meara epidermolysis bullosa simplex. *Eur J Hum Genet* 7(3):293–300.
42. Rogers GE (1985) Genes for hair and avian keratins. *Ann N Y Acad Sci* 455:403–425.
43. Bereiter-Hahn J, Matoltsy AG, Richards KS (1986) *Biology of the Integument 2 Vertebrates* (Springer, Berlin).
44. Knapp LW, Shames RB, Barnes GL, Sawyer RH (1993) Region-specific patterns of beta keratin expression during avian skin development. *Dev Dyn* 196(4):283–290.
45. Presland RB, et al. (1989) Avian keratin genes. I. A molecular analysis of the structure and expression of a group of feather keratin genes. *J Mol Biol* 209(4):549–559.
46. Presland RB, Whitbread LA, Rogers GE (1989) Avian keratin genes. II. Chromosomal arrangement and close linkage of three gene families. *J Mol Biol* 209(4):561–576.
47. Whitbread LA, Gregg K, Rogers GE (1991) The structure and expression of a gene encoding chick claw keratin. *Gene* 101(2):223–229.
48. Alibardi L, Dalla Valle L, Nardi A, Toni M (2009) Evolution of hard proteins in the sauropsid integument in relation to the cornification of skin derivatives in amniotes. *J Anat* 214(4):560–586.
49. Jarvis ED, et al. (2014) Whole-genome analyses resolve early branches in the tree of life of modern birds. *Science* 346(6215):1320–1331.
50. Ng CS, et al. (2012) The chicken frizzle feather is due to an α-keratin (KRT75) mutation that causes a defective rachis. *PLoS Genet* 8(7):e1002748.
51. Oshima RG (2007) Intermediate filaments: A historical perspective. *Exp Cell Res* 313(10):1981–1994.
52. Vaidya MM, Kanojia D (2007) Keratins: Markers of cell differentiation or regulators of cell differentiation? *J Biosci* 32(4):629–634.
53. Oriolo AS, Wald FA, Ramsauer VP, Salas PJ (2007) Intermediate filaments: A role in epithelial polarity. *Exp Cell Res* 313(10):2255–2264.
54. Pallari HM, Eriksson JE (2006) Intermediate filaments as signaling platforms. *Sci STKE* 2006(366):pe53.
55. Kim S, Coulombe PA (2007) Intermediate filament scaffolds fulfill mechanical, organizational, and signaling functions in the cytoplasm. *Genes Dev* 21(13):1581–1597.
56. Simpson CL, Patel DM, Green KJ (2011) Deconstructing the skin: Cytoarchitectural determinants of epidermal morphogenesis. *Nat Rev Mol Cell Biol* 12(9):565–580.
57. Toivola DM, et al. (2001) Disturbances in hepatic cell-cycle regulation in mice with assembly-deficient keratins 8/18. *Hepatology* 34(6):1174–1183.
58. Pan X, Hobbs RP, Coulombe PA (2013) The expanding significance of keratin intermediate filaments in normal and diseased epithelia. *Curr Opin Cell Biol* 25(1):47–56.
59. Eriksson JE, et al. (2009) Introducing intermediate filaments: From discovery to disease. *J Clin Invest* 119(7):1763–1771.
60. Ellegren H (2010) Evolutionary stasis: The stable chromosomes of birds. *Trends Ecol Evol* 25(5):283–291.
61. Li YI, Kong L, Ponting CP, Haerty W (2013) Rapid evolution of beta-keratin genes contribute to phenotypic differences that distinguish turtles and birds from other reptiles. *Genome Biol Evol* 5(5):923–933.
62. Conant GC, Wolfe KH (2008) Turning a hobby into a job: How duplicated genes find new functions. *Nat Rev Genet* 9(12):938–950.
63. Chuong CM, Chodankar R, Widelitz RB, Jiang TX (2000) Evo-devo of feathers and scales: Building complex epithelial appendages. *Curr Opin Genet Dev* 10(4):449–456.
64. Weiss IM, Kirchner HO (2010) The peacock's train (Pavo cristatus and Pavo cristatus mut. alba) I. structure, mechanics, and chemistry of the tail feather coverts. *J Exp Zool A Ecol Genet Physiol* 313(10):690–703.
65. Jiang T-X, Stott S, Widelitz RB, Chuong C-M (1998) Current methods in the study of avian skin appendages. *Molecular Basis of Epithelial Appendage Morphogenesis*, ed Chuong C-M (Landes Bioscience, Austin, TX), pp 395–408.
66. Anders S, Pyl PT, Huber W (2015) HTSeq–a Python framework to work with high-throughput sequencing data. *Bioinformatics* 31(2):166–169.
67. Robinson MD, Oshlack A (2010) A scaling normalization method for differential expression analysis of RNA-seq data. *Genome Biol* 11(3):R25.
68. Robinson MD, McCarthy DJ, Smyth GK (2010) edgeR: A Bioconductor package for differential expression analysis of digital gene expression data. *Bioinformatics* 26(1): 139–140.
69. Chuong CM, Widelitz RB, Ting-Berreth S, Jiang TX (1996) Early events during avian skin appendage regeneration: Dependence on epithelial-mesenchymal interaction and order of molecular reappearance. *J Invest Dermatol* 107(4):639–646.

Supporting Information

Wu et al. 10.1073/pnas.1520566112

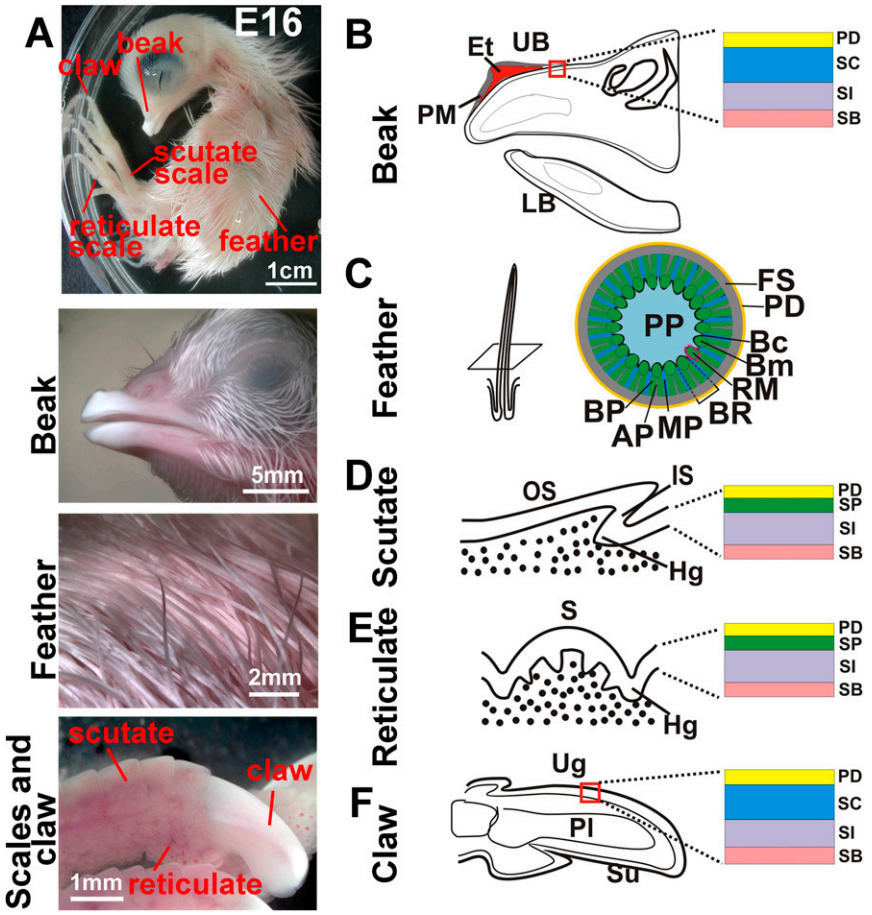

Fig. S1. The structure of different chicken skin appendages. (*A*) Bright field view of skin appendages at E16. (*B–F*) Schematic drawing of embryonic skin appendages and the layers that comprise them. (*B*) Beak. (*C*) Feather. (*D*) Scutate scale. (*E*) Reticulate scale. (*F*) Claw. AP, axial plate; Bc, barb cortex; Bm, barb medulla; BP, barb plate; BR, barb ridge; Et, egg tooth; FS, feather sheath; Hg, hinge; IS, inner surface; LB; lower beak; MP, marginal plate; OS, outer surface; PD, periderm; Pl, Phalange I; PM, periderm above the egg tooth; PP, pulp; RM, ramus; S, surface; SB, stratum basal; SC, stratum corneum; SI, stratum intermedium; SP, subperiderm; Su, subunguis; UB, upper beak; Ug, unguis.

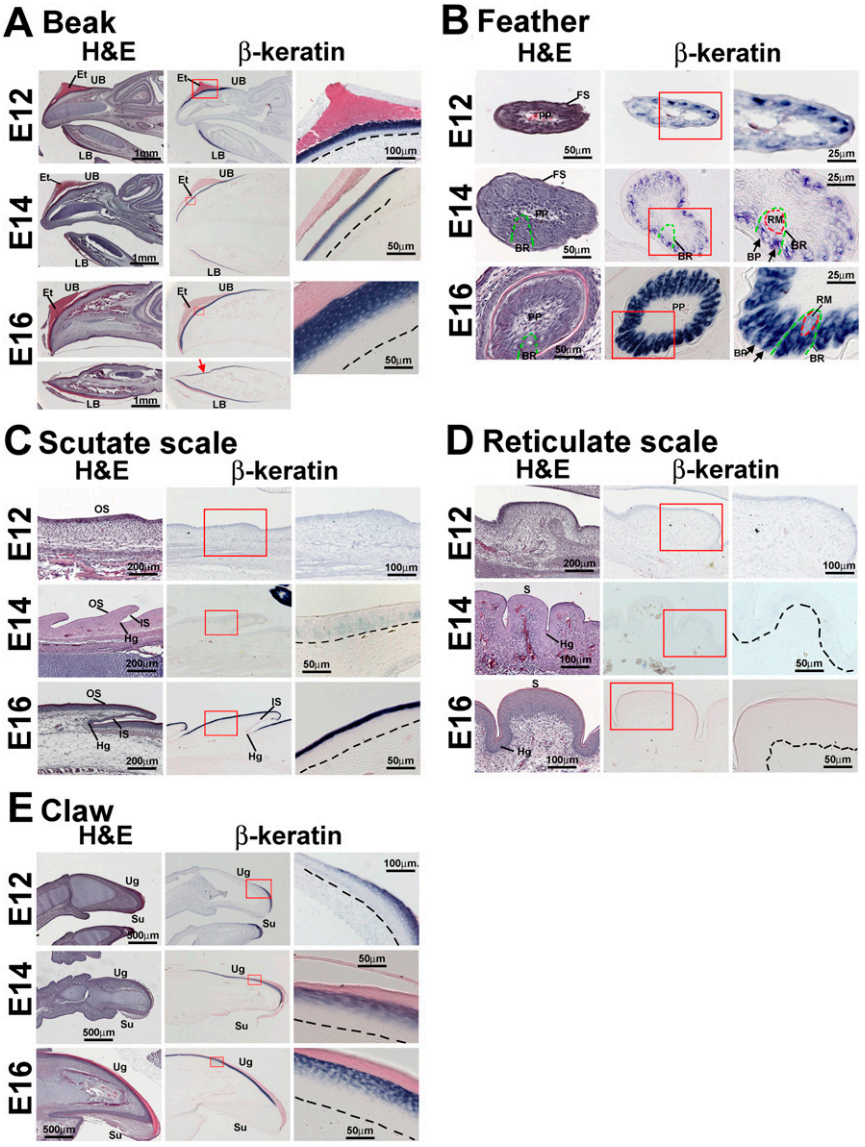

Fig. S2. The expression of common β-keratin transcripts in E12–E16 skin appendages. H&E (*Left*) and β-keratin in situ hybridization (*Middle* and *Right*, *Right* has higher magnification). E12, *Upper*; E14, *Middle*; E16, *Lower*. (*A*) Beak. (*B*) Feather. (*C*) Scutate scale. (*D*) Reticulate scale. (*E*) Claw. Black dotted line in *A* and *C–E* indicate the basement membrane. Green dotted line in *B* indicates the barb ridge. Black arrows in *B* indicate the barb plate. Red arrow in *A* indicates the oral epidermis. Red dotted circle in *B* indicates the ramus forming region. BP, barb plate; BR, barb ridge; Et, egg tooth; FS, feather sheath; Hg, hinge; IS, inner surface; LB; lower beak; OS, outer surface; PP, pulp; RM, ramus; S, surface; Su, subunguis; UB, upper beak; Ug, unguis.

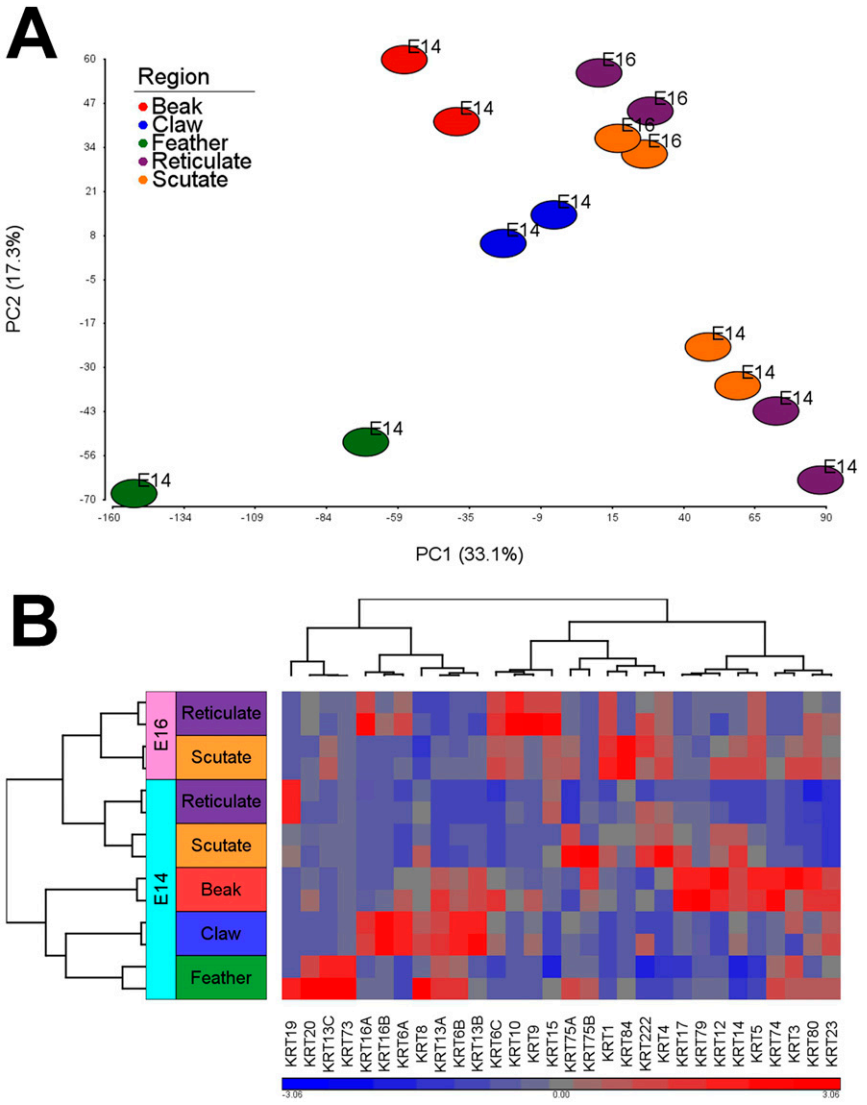

Fig. S3. RNA-seq analysis of chicken skin in different regions and developmental time. (*A*) PCA plot of RNA-seq samples for all genes. Similarities of gene expression patterns were calculated and mapped for E14 beaks, E14 feathers, E14 scutate scales, E14 reticulate scales, E14 claws, E16 scutate scales, and E16 reticulate scales. (*B*) Hierarchical clustering of α-keratin gene expression profile inferred from RNA-seq data.

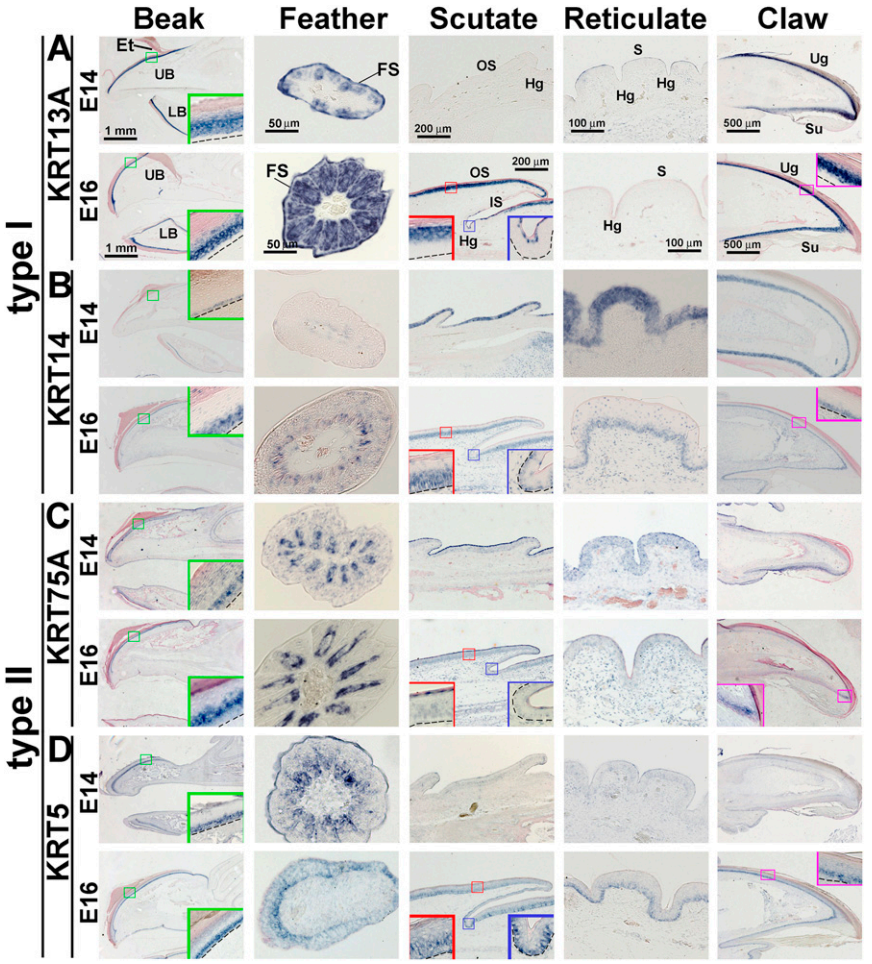

Fig. S4. In situ hybridization of four representative α-keratin transcripts in different skin appendages at E14 and E16. Type I α-keratin, KRT13A (*A*); KRT14 (*B*). Type II α-keratin, KRT75A (*C*); KRT5 (*D*). (*Upper*) E14. (*Lower*) E16. *Insets* are higher magnification views of the indicated area. Black dotted line indicates the basement membrane. Et; egg tooth; FS, feather sheath; Hg, hinge; IS, inner surface; LB, lower beak, OS, outer surface; S, surface; Su, subunguis; UB; upper beak, Ug, unguis.

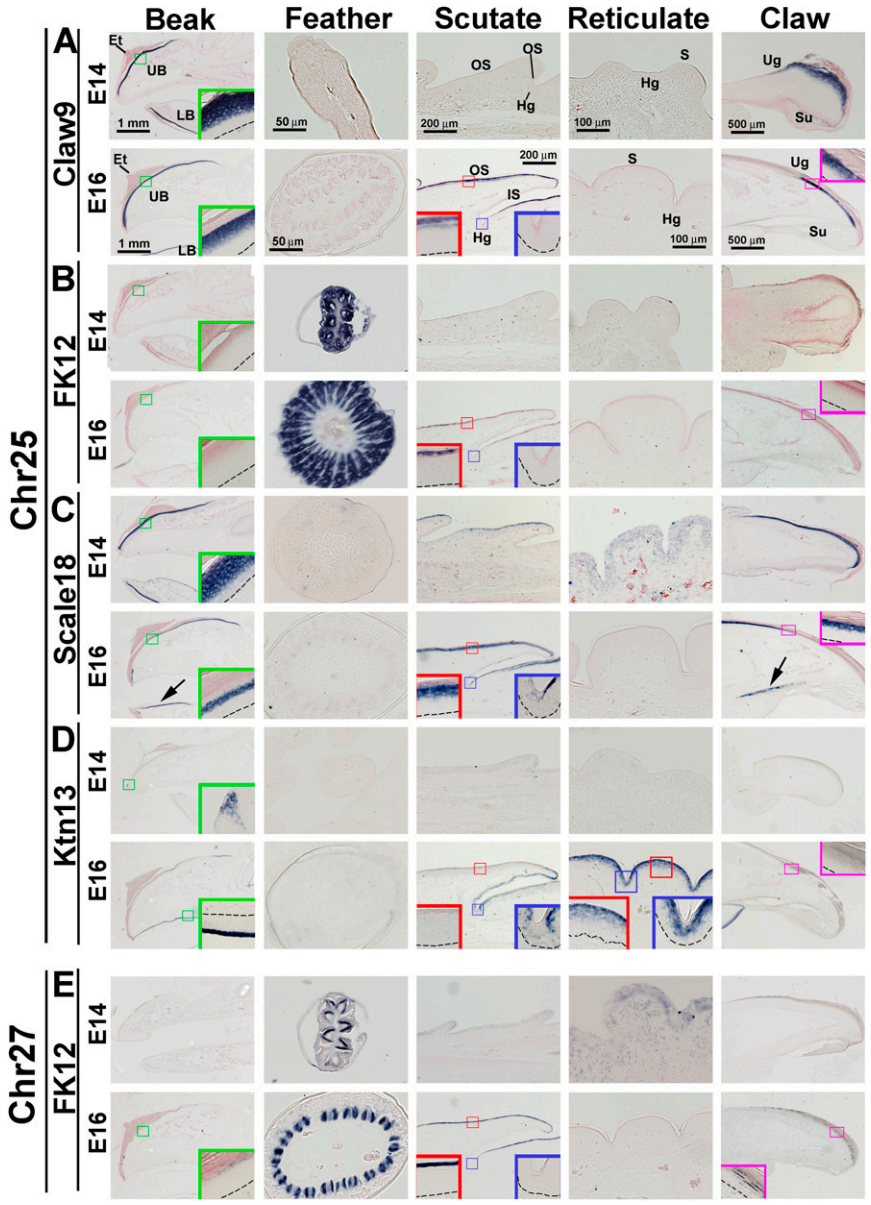

Fig. S5. In situ hybridization of five representative β-keratin transcripts encoded on Chr25 and Chr27 among different skin appendages at E14 and E16. (*A*) Chr25-Claw9. (*B*) Chr25-FK12. (*C*) Chr25-Scale18. (*D*) Chr25-F. (*E*) Chr27-FK12. Arrows in *C* indicate the expression of Scale18 in lower beak inner-oral epidermis and subunguis. (*Upper*) E14. (*Lower*) E16. *Insets* are higher magnification views of the indicated area. Black dotted line indicates the basement membrane. Et; egg tooth; FS, feather sheath; Hg, hinge; IS, inner surface; LB, lower beak, OS, outer surface; S, surface; Su, subunguis; UB; upper beak, Ug, unguis.

Table S1. List of RNA-seq samples

Stages	No. of samples
E14	
E14 Feather	2
E14 Scutate scale	2
E14 reticulate scale	2
E14 Claw	2
E14 Beak	2
E16	
E16 Scutate scale	2
E16 reticulate scale	2

Table S2. List of probes used for in situ hybridization

Probes used in this paper	Probes name used in ref. 25	Forward primer	Backward primer	PCR size, bp
Common probes				
Common α type II	Common α type II	CGACAACAAATTTGCCTCCT	CATCTGCCTTGGCCTGTAGT	359
Common β-keratin	Common β-keratin	ATGTCCTGCTCCAACCTC	GGGGAAGGAGCTGAGGAT	156
Specific probes				
α type I				
KRT13A	KRT17	CGGGCTAGGAGATGACACAG	CATCAGGCAGAAGCACAGTT	251
KRT14	KRT14	CTCATCCCGTGAGCAGATG	GCTTTATTAAATGTGTACAGAATGCAC	173
α type II				
KRT5	KRT5	GCAACGTGCTGTCTTACCAA	GATGTGAGTAGGGGCTTCCA	393
KRT75A	KRT75	CTCCCTCACCAGAAAACACC	GACAAACACCAGAGAGTGAAGAGA	302
β-keratin (Chr25)				
Claw9	Claw4	CTCTGTCCGTGGTTGAAGAAG	AGAGGGCAGAGGGACAGG	230
FK12	FK14	TGAGGTGGACATCCTGTGAA	A CAATGGGATGCCTGACTTC	329
Scale18	Scale5	ATCTCACATGAAGGCCCAAG	TGTTTCCAGACAGTTCCAGAGA	309
Ktn13	N/A	AGCCAATGTCTCCCATTCC	TCAGCCAGCTGCATGAATAC	200
β-keratin (Chr27)				
FK12	FK12	GCCATGATCCTGGTGAAATC	AGCTCATGCAAGGCTTGTG	316